Asociación Argentina de Mecánica Computacional

Mecánica Computacional Vol XXVII, págs. 941-958 (artículo completo)
Alberto Cardona, Mario Storti, Carlos Zuppa. (Eds.)
San Luis, Argentina, 10-13 Noviembre 2008

INTEGRATED ANALYSIS OF TIME-DEPENDENT FAILURE USING A VISCOPLASTIC THEORY

Ricardo H. Lorefice[a], Guillermo Etse[b], Marcia B. Rizo Patron[a]

[a]CMAE - Universidad Nacional de Santiago del Estero,
(4200) –Santiago del Estero, ARGENTINA rlorefice@gmail.com
[b]CEMNCI -UNT- CONICET
(4000) – Tucuman, ARGENTINA getse@herrera.unt.edu.ar

Key words: Viscoplasticity, Dynamic yield surfaces, Constitutive modeling.

Abstract. The implications of using a viscoplastic theory to study time-dependent failure in solid materials are analyzed considering the elasto-viscoplastic theory of Perzyna (1963, 1966). The crucial aspect is that a viscoplastic failure surface has an intrinsically dynamic nature, which allows us to take advantage of the postulate of maximum dissipation to use a unique formulation to investigate a wide range of engineering problems like dynamic loading, creep or relaxation. Also, the consequences of formulate constitutive models that includes hardening, perfect and softening viscoplasticity are also addressed in the framework of a unique and consistent strategy.

1. INTRODUCTION

In the last years, various viscoplastic models have been proposed. A widely-used viscoplastic formulation is the Perzyna model (Perzyna, 1963; Perzyna, 1966). The main feature of this model is that the inviscid yield function used for describing the viscoplastic strain can become larger than zero, which effect is known as *overstress*. The characteristics of the Perzyna model have been addressed by several authors (Sluys, 1992; Cristescu, 1994; Cristescu and Cazacu, 2000; Ponthot, 1995; Wang, 1997; Wang et al. 1997; Carosio et al., 2000; Carosio, 2001; Etse and Willam, 1999). Perzyna's model has been widely used to capture rate-dependent effects in solid materials, like Luders bands and the Portevin-Le Chatelier effect in metals (Wang, 1997; Wang et al. 1997), shear banding and creep in geomaterials (Desai and Zhang, 1987; Cristescu and Cazacu, 2000) and to analyze localization and bifurcation properties (Willam et al. 1993; Etse et al. 1997).

Alternatively to the original proposal of Perzyna (1963; 1966), viscoplasticity can be modeled by direct incorporation of the time-dependency in a yield function which, together with the consistency parameter, obeys the classical Kuhn-Tucker relations. Recently, the *consistency model* has been proposed (Wang, 1997; Wang et al. 1997) in which a rate-dependent yield surface is defined. Furthermore, other authors have considered a rate-dependent yield formulation in combination with coupling to damage (Mahnken et al, 1998; Johansson et al. 1999). Very recently, the implications of the concept of a dynamic rate-dependent yield surface have been also investigated (Ristinmaa and Ottosen, 2000). Several authors extended cohesive-frictional formulations like the parabolic Drucker-Prager model (Carosio et al. 2000; Carosio 2001) and the Extended Leon model for concrete (Etse and Willam, 1999; Etse et al. 1997) to take into account rate/time effects.

Ponthot (1995), proposed an interesting viscoplastic formulation, the so-called *continuous viscoplasticity*. This approach, with few modifications, preserves the validity of the well-known format of elastoplasticity theory, capturing all the relevant aspects of rate-dependent materials. In this model, the consistency condition for the yield function is enforced and therefore, numerical algorithms similar to the Closest Point Projection Method from rate independent plasticity can be adopted. Thus, robust and efficient numerical procedures can be utilized, making this model attractive from a numerical point of view.

In this context, Perzyna's overstress theory provides a unified approach to analyze a wide range of engineering problems, from quasi-static to dynamic failure of building materials, prediction of creep strains, stress relaxation and delayed rupture. Moreover, as pointed out for many authors, viscoplasticity theory can be viewed as a regularization of the classical rate-independent elastoplastic theory, and it may be proven that a viscoplastic formulation can be viewed as the optimality conditions of a regularized penalty functional, with penalty parameter $1/\eta > 0$ of the maximum plastic dissipation function. According to this interpretation of the viscoplastic regularization concept, for decreasing values of the viscosity parameter η, in the limit as $\eta \to 0$ the inviscid formulation is recovered. In the next section, the continuous-viscoplasticity concept will be used to formulate a rate-dependent interface model on the basis of Perzyna's theory.

2. RATE DEPENDENT CONTINUOUS FORMULATION

Similar to the flow theory of plasticity, the constitutive relations for Perzyna's type elasto- viscoplastic material formulations may be written as

$$\dot{\boldsymbol{\sigma}} = \dot{\boldsymbol{\sigma}}_e - \dot{\boldsymbol{\sigma}}_{vp} = \mathbf{E} : (\boldsymbol{\varepsilon} - \boldsymbol{\varepsilon}_{vp}) \tag{1}$$

$$\boldsymbol{\varepsilon}_{vp} = \mathbf{g}(\psi, F, \boldsymbol{\sigma}) = \frac{1}{\eta}\langle \psi(F) \rangle \mathbf{m} \tag{2}$$

$$\mathbf{m} = \mathbf{A} : \mathbf{n} = \mathbf{A} : \frac{\partial F}{\partial \boldsymbol{\sigma}} \tag{3}$$

$$\psi(F) = \left[\frac{F(\boldsymbol{\sigma}, \mathbf{q})}{F_0} \right]^N \tag{4}$$

$$\dot{\mathbf{q}} = \frac{1}{\eta}\langle \psi(F) \rangle \mathbf{H} : \mathbf{m} \tag{5}$$

whereby $\boldsymbol{\varepsilon}_{vp}$ represents the viscoplastic portion of the total strain tensor **e**, η the viscosity and **q** the set of hardening/softening variables defined as a tensor of arbitrary order. Relation (1) follows the additive decomposition of the total strain rate into an elastic and a viscoplastic part $\boldsymbol{\varepsilon} = \boldsymbol{\varepsilon}_e + \boldsymbol{\varepsilon}_{vp}$, quite similar to the Prandtl-Reuss equations in case of inviscid elasto-plastic constitutive relations. Eq. (2) and (3) describe a general non-associated flow rule, whereby the direction of the viscoplastic strains **m**, is obtained by a modification of the gradient tensor **n** of the yield surface *F* by means of the fourth order transformation tensor ***A***. Moreover, $\psi(F)$ is a dimensionless monotonically increasing over-stress function whereby F_0 represents a normalizing factor, tipically chosen as the initial strength threshold. The power *N* in Eq. (4) defines the order of the Perzyna's viscoplatic formulation. Higher values of the exponent *N* leads to more rate-sensitive models, while the McCauley brackets in Eq. (2) defines the features of the over-stress function as

$$\langle \psi(F) \rangle = \begin{cases} F & \text{if } F > 0 \\ 0 & \text{if } F \leq 0 \end{cases} \tag{6}$$

being $F = F(\boldsymbol{\sigma}, \mathbf{q})$ a convex yield function which defines the limit of the elastic domain. Finally eq. (5) represents the evolution law of the hardening/softening variables **q** by means of a suitable tensorial function of the state variables, ***H***. In the continuous formulation, eqs. (1) to (5) are complemented by a consistency parameter $\dot{\lambda}$, defined as an increasing function of the over-stress

$$\dot{\lambda} = \frac{\langle \psi(F) \rangle}{\eta} \tag{7}$$

So that the evolution equations (2) and (5) take now the classical forms

$$\dot{\boldsymbol{\varepsilon}}_{vp} = \dot{\lambda}\mathbf{m} \tag{8}$$

$$\dot{\mathbf{q}} = \dot{\lambda}\mathbf{H} : \mathbf{m} = \dot{\lambda}\mathbf{h} \tag{9}$$

being $\mathbf{h} = \mathbf{H}:\mathbf{m}$. Thus, from eqs. (2) and (8) follows

$$F = \psi^{-1}\left(\frac{\|\boldsymbol{\varepsilon}_{vp}\|}{\|\mathbf{m}\|}\eta\right) = \psi^{-1}(\dot{\lambda}\eta) \tag{10}$$

We may now define for the viscoplastic range, the new constraint condition

$$\overline{F} = F - \psi^{-1}(\dot{\lambda}\eta) = 0 \tag{11}$$

which represent a generalization of the inviscid yield condition *F=0* for rate-dependent Perzyna viscoplastic materials. The name *continuous formulation* is due to the fact that the condition $\eta = 0$ (without viscosity effect) leads to the elastoplastic yield condition *F=0*. Moreover, from eq. (7) follows that when $\eta \to 0$ the consistency parameter remains finite and positive since also the over-stress goes to zero. The other extreme case, $\eta \to \infty$ leads to the inequality $\overline{F} < 0$ for every possible stress state, indicating that only elastic response may be activated. The constraint condition defined by Eq. (11) allows a generalization of the Kuhn-Tucker conditions which may be now written as

$$\dot{\lambda}\overline{F} = 0 \qquad \dot{\lambda} \geq 0 \qquad \overline{F} \leq 0 \tag{12}$$

Finally, the viscoplastic consistency condition expands into

$$\dot{\overline{F}} = \mathbf{n} : \dot{\boldsymbol{\sigma}} + \overline{\mathbf{r}}\dot{\mathbf{q}} - \frac{\partial \psi^{-1}(\dot{\lambda}\eta)}{\partial \dot{\lambda}}\ddot{\lambda} = 0 \tag{13}$$

where

$$\overline{\mathbf{r}} = \frac{\partial \overline{F}}{\partial \mathbf{q}} = \frac{\partial F}{\partial \mathbf{q}} - \frac{\partial \psi^{-1}(\dot{\lambda}\eta)}{\partial \mathbf{q}} \tag{14}$$

Other recent and interesting approach to this problem (Wang 1997; Wang et al. 1997) includes the strain rate as state variable into the flow and viscoplastic potential function, i.e.

$$F^{vp} = F^{vp}(\boldsymbol{\sigma}, \mathbf{q}, \boldsymbol{\varepsilon}) \tag{15}$$

which also leads to a rate dependent Kuhn-Tucker conditions as in case of the continuous Perzyna formulation.

3. VISCOPLASTIC INTERFACE LAW

In this section the rate-dependent extension of the interface model by Carol et al. (1997) and Lopez (1999) is summarized. The viscoplastic yield condition of the interface constitutive model can be expressed as (Etse et al. 2004a, 2004b; Lorefice et al. 2006; Lorefice et al. 2007; Lorefice 2007; Lorefice et al. 2008)

$$\overline{F} = \sigma^2 - (c - \tau tg\phi)^2 + (c - \chi tg\phi)^2 - (\dot{\lambda}\eta)^{1/N} \tag{16}$$

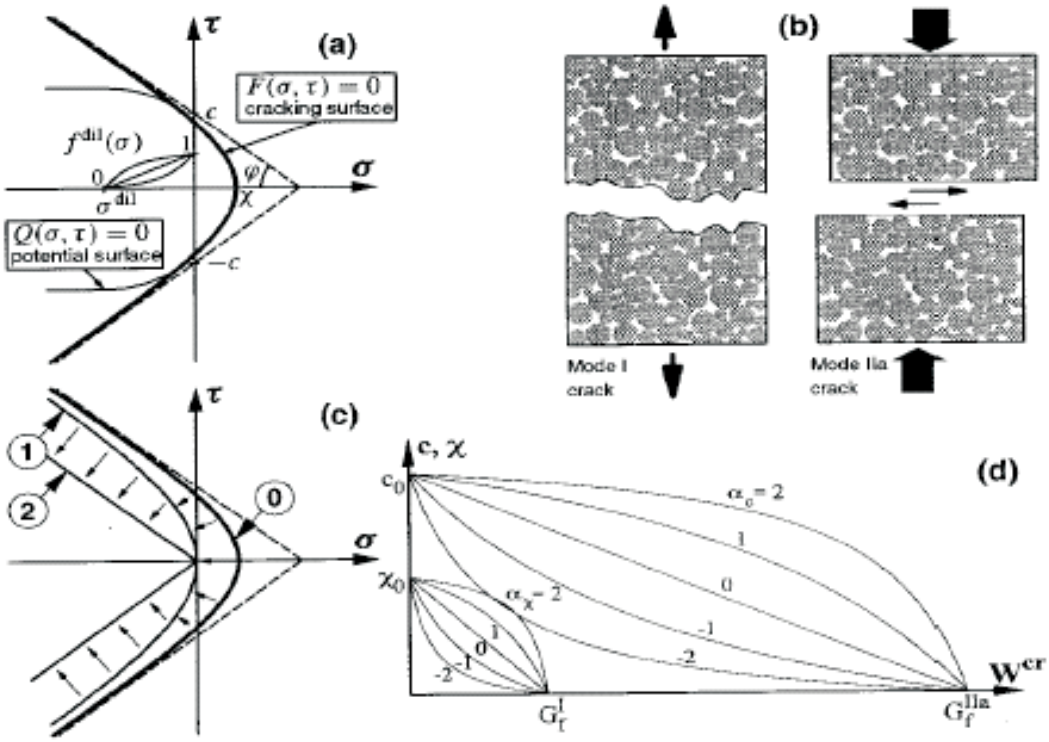

Figure 1: Hyperbolic failure surface - inviscid model

being σ and τ the normal and tangential stress components at the interface with χ the traction strength (vertex of hyperbola), c the apparent cohesion (shear strength) and ϕ the friction angle. The energy dissipated during the time-dependent fracture process is defined as

$$dW^{vcr} = \sigma\, du^{vcr} + \tau dv^{vcr} \quad \text{if} \quad \sigma \geq 0 \tag{17}$$

$$dW^{vcr} = \tau dv^{vcr}\left(1 - \left|\frac{\sigma \mathrm{tg}\phi}{\tau}\right|\right) \quad \text{if } \sigma < 0 \tag{18}$$

Whereby u^{vcr} and v^{vcr} are the normal and tangential (critical) rate-dependent rupture displacements, respectively. The viscoplastic flow is fully associated in tension while non-associated in compression, according to

$$\mathbf{m} = \mathbf{A} : \mathbf{n} \tag{19}$$

$$\mathbf{n} = \frac{\partial F}{\partial \boldsymbol{\sigma}} = \begin{bmatrix} \dfrac{\partial F}{\partial \sigma} \\ \dfrac{\partial F}{\partial \tau} \end{bmatrix} = \begin{bmatrix} 2tg\phi(c - \sigma tg\phi) \\ 2\tau \end{bmatrix} \tag{20}$$

$$\mathbf{A} = \begin{bmatrix} 1 & 0 \\ 0 & 1 \end{bmatrix} \quad \text{if } \sigma > 0 \tag{21}$$

and

$$\mathbf{A} = \begin{bmatrix} f_{\sigma}^{dil} f_{c}^{dil} & 0 \\ 0 & 1 \end{bmatrix} \quad \text{if } \sigma < 0 \tag{22}$$

being **A** a transformation matrix, **n** the gradient to the viscoplastic yield surface and **m** the gradient to the viscoplastic potential function. The factors f_c^{dil} and f_σ^{dil} accounts for the dilatancy effects in the compressive regime by means of a reduction of the interface normal component of the stress tensor. The continuum viscoplasticity form of the rate dependent interface constitutive model is defined by the following set of equations:

$$\dot{\mathbf{u}} = \dot{\mathbf{u}}^{e} + \dot{\mathbf{u}}^{vcr} \tag{23}$$

$$\dot{\mathbf{u}}^{e} = \left(\mathbf{E}\right)^{-1} \dot{\boldsymbol{\sigma}} \tag{24}$$

$$\dot{\boldsymbol{\sigma}} = \mathbf{E}(\mathbf{u} - \mathbf{u}^{vcr}) \tag{25}$$

where $\dot{\mathbf{u}}$ are the rate of the relative displacements which are decomposed into an elastic $\dot{\mathbf{u}}^{e}$ and a viscoplastic component $\dot{\mathbf{u}}^{vcr}$, **E** is the elastic stiffness matrix which has a diagonal structure with non-zero terms equal to the constant assumed normal and shear stiffnesses $E_N = E_T$. The non-linear system of equations is solved using a Newton-Raphson iterative procedure in the framework of the Closest Point Projection Method (CPPM) starting from the rate-dependent consistency condition which takes the form

$$\dot{\bar{F}} = \mathbf{n}^{T} \cdot \dot{\boldsymbol{\sigma}} - \bar{r}_i \dot{q}_i - \frac{1}{N} \eta (\eta \dot{\lambda})^{1/N-1} \tag{26}$$

with

$$\bar{r}_i = \frac{\partial F}{\partial q_i} \frac{\partial q_i}{\partial W^{vcr}} \quad \text{and} \quad \dot{q}_i = \frac{\partial W^{vcr}}{\partial \mathbf{u}^{vcr}} \mathbf{m} \dot{\lambda} \tag{27}$$

Thereby, the parameters q_i of the yield surface, which evolves during the softening branch, are in this case χ, c, while ϕ remains constant (see Figure 1)

4. APPLICATION: BASIC CREEP/RELAXATION ANALYSIS

4.1 Constitutive level – relaxation test

In this section numerical examples are presented at constitutive level. They are intended to illustrate model performance to simulate time dependent failure processes. Two different types of loadcases are examined here: a) A constant normal displacement is applied as showed in Figure 2 (a), which resulted to a constant strain state. The applied displacements are chosen in such a way that the corresponding internal stress state to be above the yield limit. In this case, the way that the stresses develop with respect to time is of interest. Usually such a loadcase goes by the name relaxation. (b) A constant force is applied to the model, see Figure 2 (b), which results to a constant stress state. The magnitude of the force is taken to be such, that the resulting stresses exceed the yield limit. Our interest in this case is to study the evolution of the displacements with respect to time. This model corresponds to that frequently found in the literature as creep case.

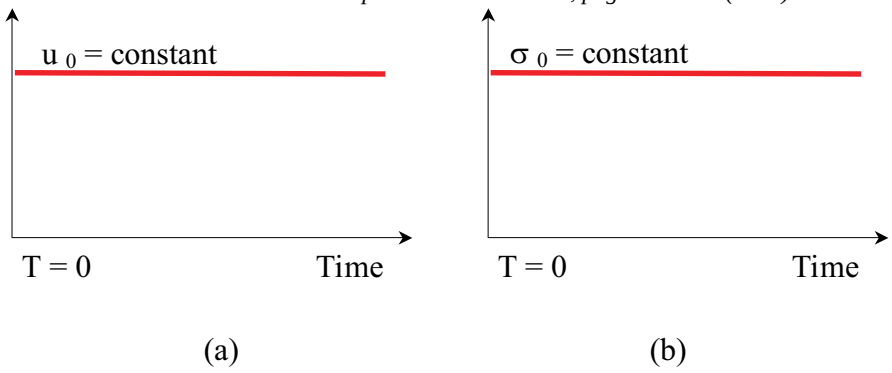

Figure 2: Constitutive tests: a) Relaxation b) Creep

In the following we will further explore the relaxation test for the following set of material parameters: E_N = 1.E7 MPa/m, χ_0 = 2.0 MPa, G_f^I = 0.00003 MPa.m, $G_f^{II} = 10G_f^I$. For these parameters the yield limit in pure traction is χ_0 = 2.0 MPa; therefore a displacement of 3.E-7 m was applied which corresponds to a uniform stress state of 3.0 MPa. The results of the elastoplastic and the elasto-viscoplastic computations are shown in Figure 3.

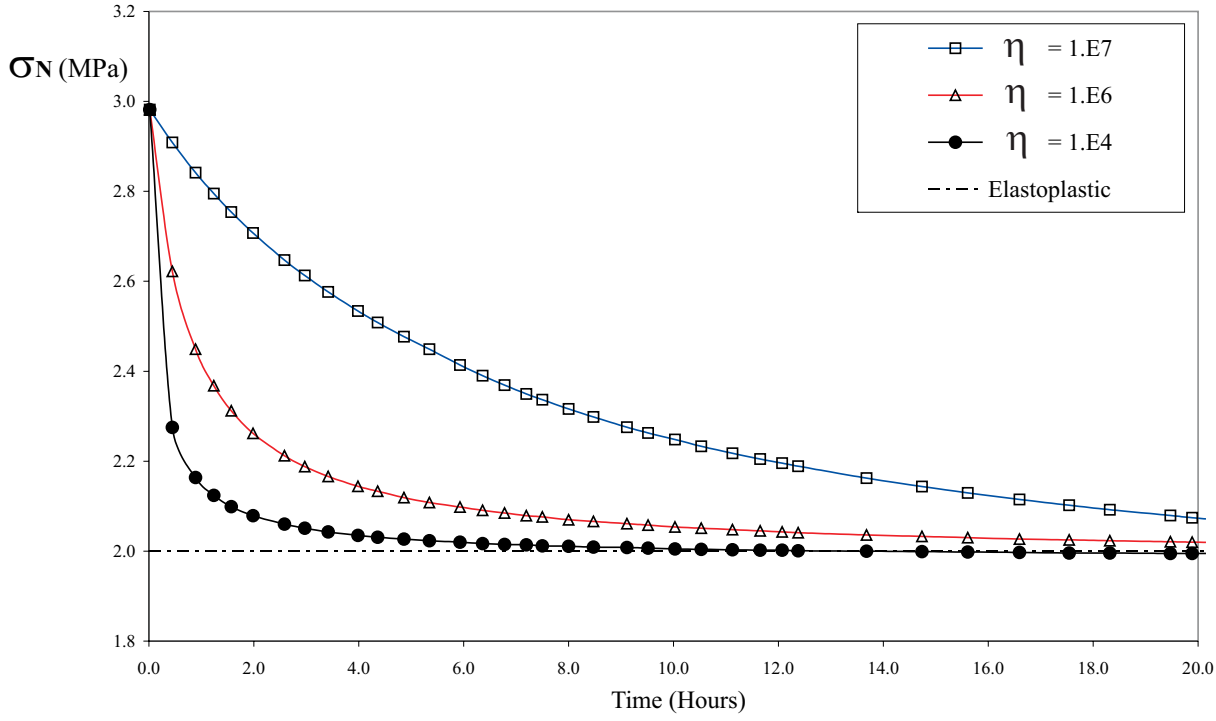

Figure 3: Relaxation test – constitutive level

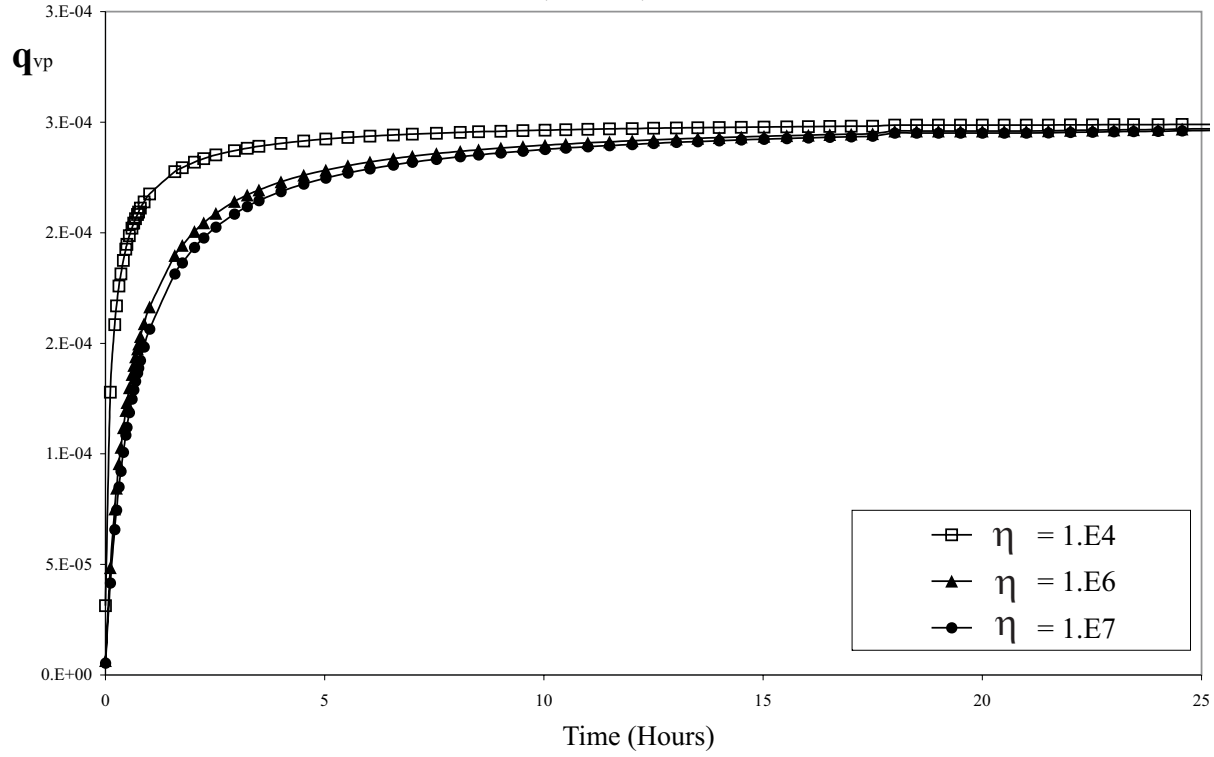

Figure 4: Relaxation test – evolution of state variable

In the same figure several cases are also plotted for different values of the viscosity parameter η. In this loadcase one may find interesting that the stresses cannot exceed the yield limit in the case of an elastoplastic material, while in the case of viscoplasticity it is in general allowed, to exceed this limit. In other words, the stresses that are developed at the interface in the case of viscoplasticity are allowed to be larger than the yield limit χ_0. This is a big advantage of viscoplasticity, since from the numerical point of view it can provide a better, more stable and reliable algorithm. From the engineering point of view it also provides a behavior coming closer to the terms, of short term and long term load carrying capacity. The evolution of the state variable is illustrated in figure 4. Also, for higher values of the viscosity parameter, higher times are needed to reach the limit value. In Figure 5 we compare the viscoelastic solution from a Maxwell chain versus the viscoplastic one for a natural relaxation time t* = η/E = 1. For this case and for comparison purposes, we introduce here two variants of the original model: a perfect viscoplastic model (with a plastic modulus $H_p = 0$), and a hardening version (setting $H_p > 0$). We can see that while for perfect viscoplasticity the numerical solution relax the stress state until reach the elastoplastic strength limit, the viscoelastic case has no limit and spread to relax the stress state to zero. Furthermore, is clear the physical meaning of the viscosity parameter η, concerning the time that the system needs to relax the stress state until reach the final, elastoplastic solution. In the same plot the hardening and softening relaxation cases are also included. Contrarily to the perfect viscoplasticity case in which the stress state evolves until reach the strength limit, for the softening/hardening cases, the stress state returns to a different stress level that depends on the value of the plastic modulus H_p.

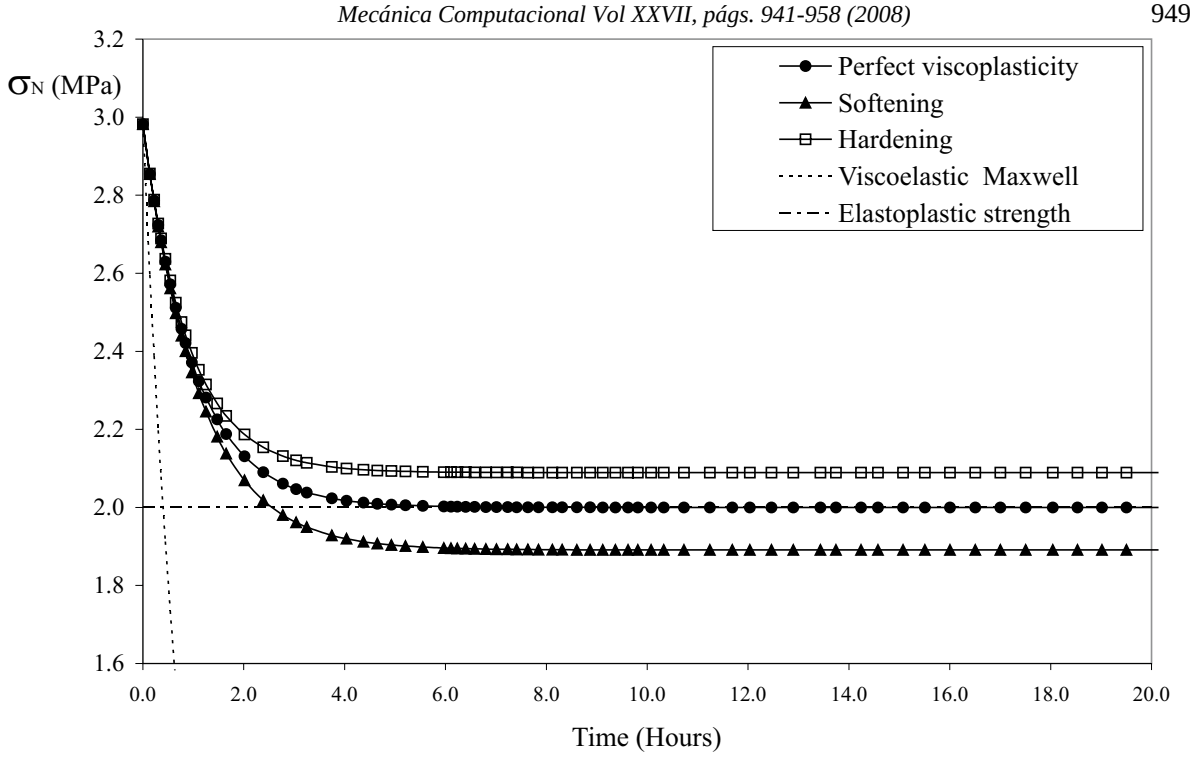

Figure 5: Comparison of different models for identical t*=η/E

In the softening case, $H_p < 0$ which leads the stress state to return to a "softened" or contracted yield surface, below the initial strength limit, and conversely, in the hardening regime the relaxation process returns the stress state to a "hardened" or expanded yield envelope above the original strength limit. We will return on this subject when analyze the creep case. From a physical standpoint, it is important to realize that the controlling factor in the relaxation process is the relative time t/t*. The absolute time $t \in [0;1)$ is regarded to be short or long only when compared with $t^* = \eta/E_n$. Equivalently, what counts is the ratio of the viscosity η in the dashpot to the stiffness E_n in the spring of the elastoviscoplastic device. Because of this, t* is also referred to as the natural relaxation time.

4.2 Constitutive level – creep test

We explore now the creep test for the same set of material parameters and for the softening case. At time t = 0, a constant load is applied to impose a traction stress state just above the elastoplastic yield limit, see figure 6. The evolution of normal displacements u_N are plotted against time for several values of the viscosity parameter η. After the stress state reaches the limit strength, the softening formulation is activated together with the creep process. This is the reason for the increasing slope of the displacement rate. For large values of the viscosity parameter η, the slope of the displacement rate decreases and the creep process is stabilized, while for smaller values we see that the process is accelerated, reaching large values of the creep displacement and tending to an almost vertical slope. This fact can also be explained considering a simple uniaxial case corresponding to an elasto-viscoplastic material, see figure 7. As discussed above, the continuous viscoplasticity formulation allows to recover the static stress-strain response in the limit when the prescribed total strain rate is very slow (or when the viscosity parameter $\eta \to 0$).

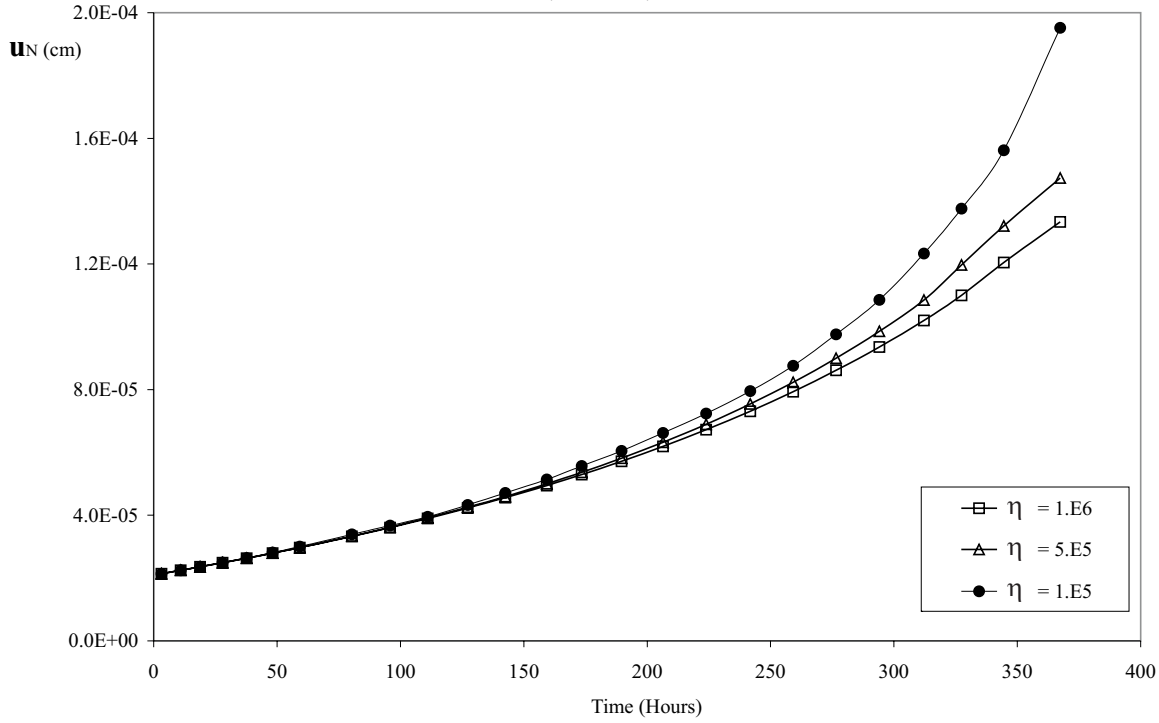

Figure 6: Creep curves - constitutive level

For stress states on this curve, the static yield condition is fulfilled, i.e. $F(\boldsymbol{\sigma},\mathbf{q}) = 0$. Hence, assume that the loading history in some way has bought us to point *A* or point *C* and consider then the following response when the stress state is held constant. In both cases, the viscoplastic strain will increase. Starting at point *A* located above the rising part of the static stress-strain curve, the point defined by (σ,ε) will move and eventually be located at point *B* on the static stress-strain curve and the total viscoplastic strain is bounded.

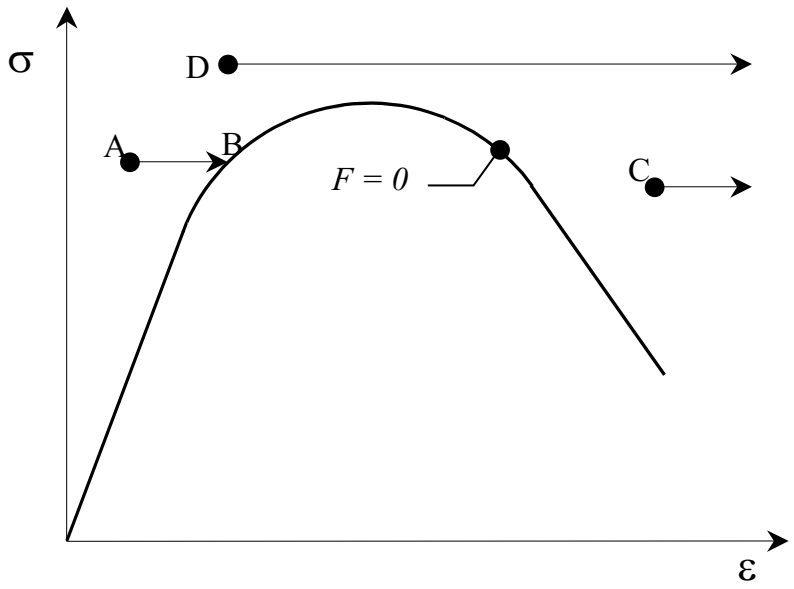

Figure 7: Typical static σ-ε curve

However, starting at point *C* located above the falling part of the static stress-strain curve (i.e. on the softening branch), the increasing viscoplastic strain will move the point (σ,ε) more and more away from the static stress-strain curve; therefore, the total viscoplastic strain is now unbounded. These results indicate that an isolated softening-based interface cannot be able to simulate the experimentally observed behavior in quasi-brittle materials under sustained loads, because a real material tends to a definite strain limit with time. However, since our intent is to investigate the capabilities of the rate-dependent interface model to capture delayed rupture in concrete and mortar materials in the framework of a discrete or explicit approach using the finite element method, hereafter we analyze the response of a viscoplastic model using a simple finite element mesh composed of two quadrilateral continuum elements and a zero-thickness continuous four-nodes interface element between them, see figure 8.

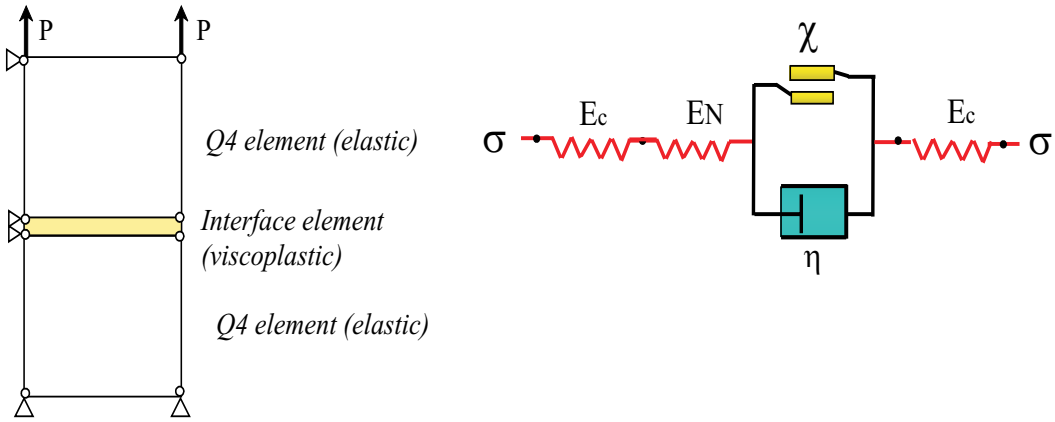

Figure 8: a) Finite element arrange b) Rheological device

The continuum elements obey an elastic constitutive law while the interface element is equipped with the viscoplastic-softening based law previously described. The creep test is carried out applying a constant traction load at the top nodes of the mesh until activate the creep mechanism. Figure 9 shows the influence of the continuum elements stiffness in the numerical response for three values of the relation E_N/E_C, being E_N the normal stiffness of the interface element and E_C the elastic stiffness of the continuum elements. The viscosity parameter was set to η =1.E7 MPa.seg and the material parameters for the interface are the same as in the constitutive example. In order to avoid the generation of spurious stress states at the interface as a result of the interaction with the continuum elements, a null value of the Poisson modulus was assigned to the continuum elements. The plot shows that for a large value of the relation E_N/E_C normal creep displacement is unbounded in similar way to the constitutive test presented in figure 6, showing an acceleration of the displacement rate and taking almost a vertical slope. For smaller values of the stiffness factor E_N/E_C a stabilizing effect is obtained, and the creep displacement turns bounded. For E_N/E_C =0.4 or E_N/E_C = 4, the final value of the creep displacement reaches a lightly different value, being the stabilizing time shorter for E_N/E_C = 0.4. Clearly, for certain values of the relation E_N/E_C, the elastic stiffness of the continuum elements acts restricting the displacement in the dashpot at the viscoplastic device (see figure 9), generating the stabilization of the overall response. This is a key aspect, because at mesomechanical level of observation, the interface elements equipped with the viscoplastic cracking law will always interact together with the continuum elements

representing the matrix or aggregates phases of concrete mesostructure. In the following, the simple finite element model previously presented will be used to investigate the numerical response of the viscoplastic interface model under different loading conditions.

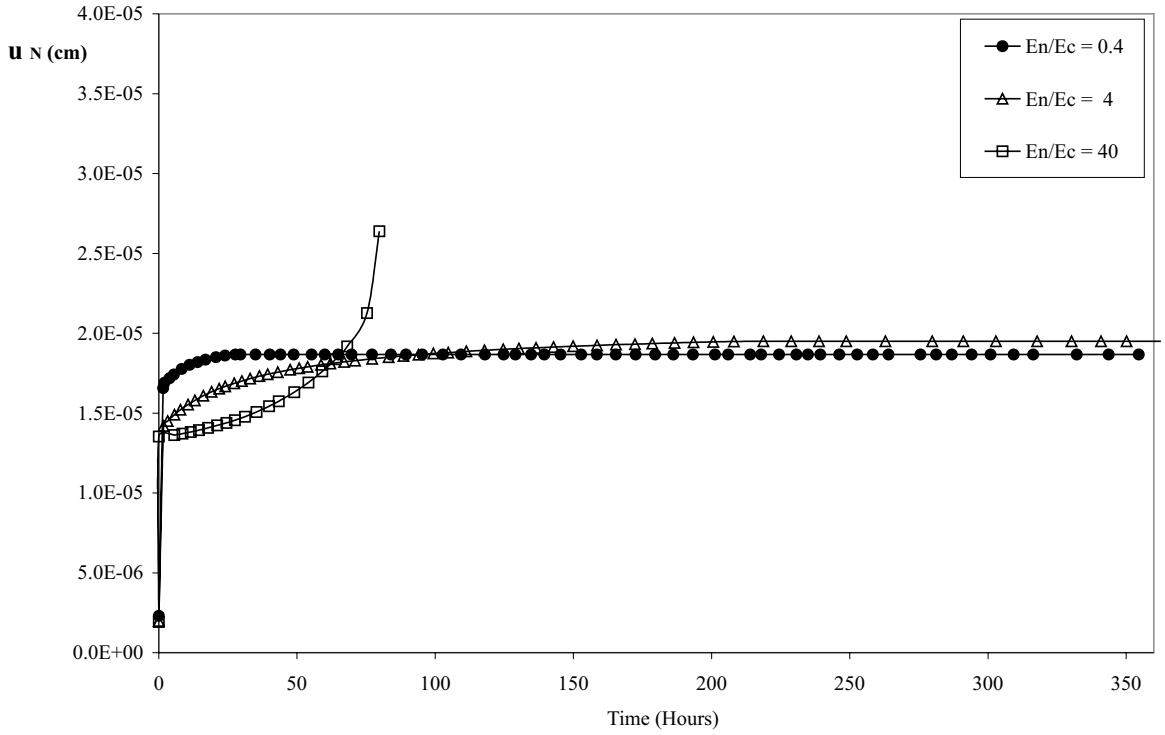

Figure 9: Creep test at Finite element level - Influence of continuum elements stiffness

The numerical results for the elastoplastic and the elastoviscoplastic model, together with several other cases for different values of the viscosity η are plotted in figure 10. What can be first noticed is that, the elastoplastic model, as expected shows no time influence; however it sets the limit for the viscoplastic solution. Secondly, the viscosity parameter is of great significance while studying a viscoplastic case: it determines the delay in time needed to reach the elastoplastic solution. In the case that the yield strength was also set to zero the response is that of a Maxwell solid, used to simulate viscoelastic materials. Figure 11 shows the sensitivity to the applied stress level in the creep case. We can see that for the lower stress level (0.6χ and 0.7χ) the delayed displacements reaches a limit value, but under a higher level of 0.8χ the delayed displacements are unbounded. This behavior is coherent with the stress evolution in time showed in figure 12, where we can see that for the higher load level the stress state reaches a peak and then falls with a negative constant slope. This behavior corresponds to a softening response at the interface and with a negative value of the plastic modulus H_p, while in the other cases the plastic modulus remains positive. In the previous examples one speaks of plastic, i.e. irreversible deformations. Once the viscoplastic mechanism is activated then some plastic deformation will remain in case of unloading. The important thing though when adopting a viscoplastic material model, is that the remaining deformation is not always that of an elastoplastic model. Depending on the time of unloading, just a portion of the plastic deformation is activated. This is illustrated by the next examples. Consider the creep case with the same material properties as defined before. At time t = 0 a load of 1.2 KN is applied and after a $t = t_1$ hours this load is removed, see figure 13.

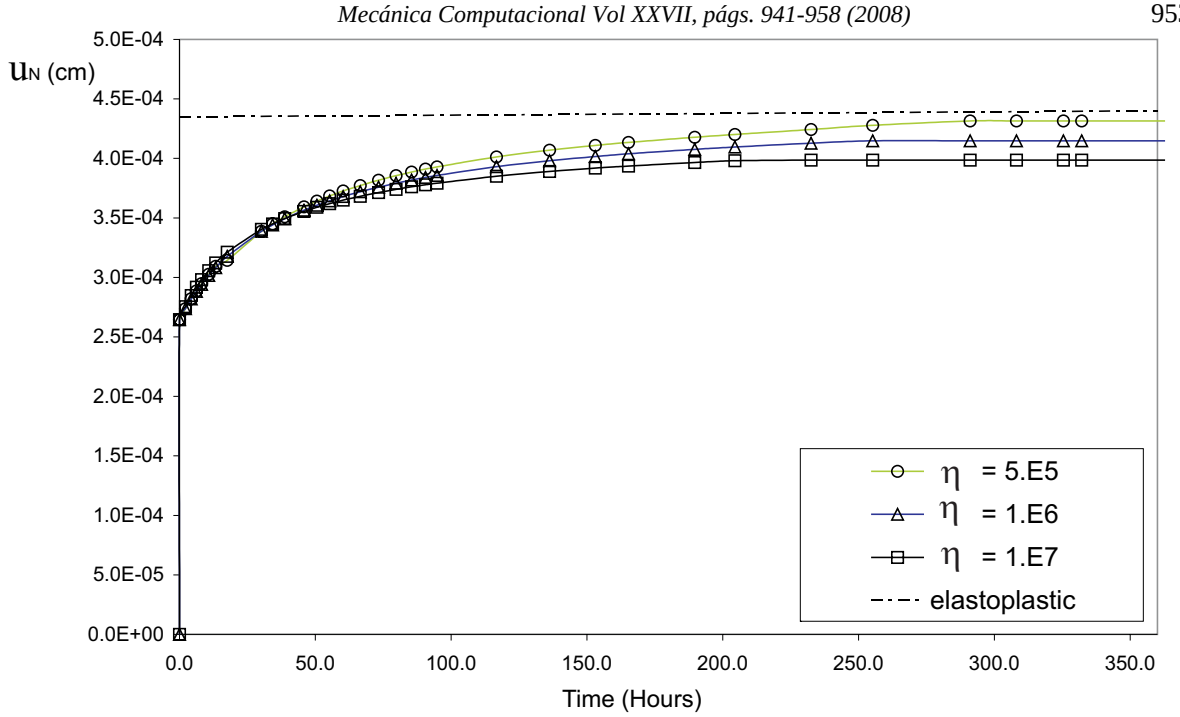

Figure 10: Creep test at Finite element level - Influence of continuum elements stiffness

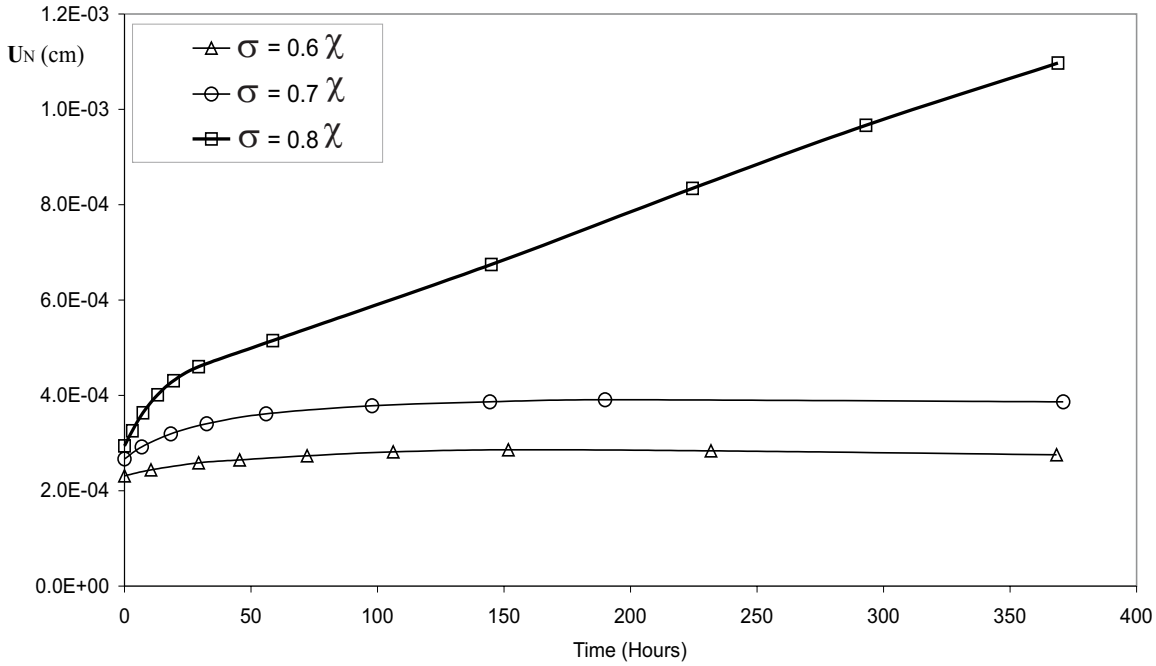

Figure 11: Creep test - Influence of stress level for η=1.E7

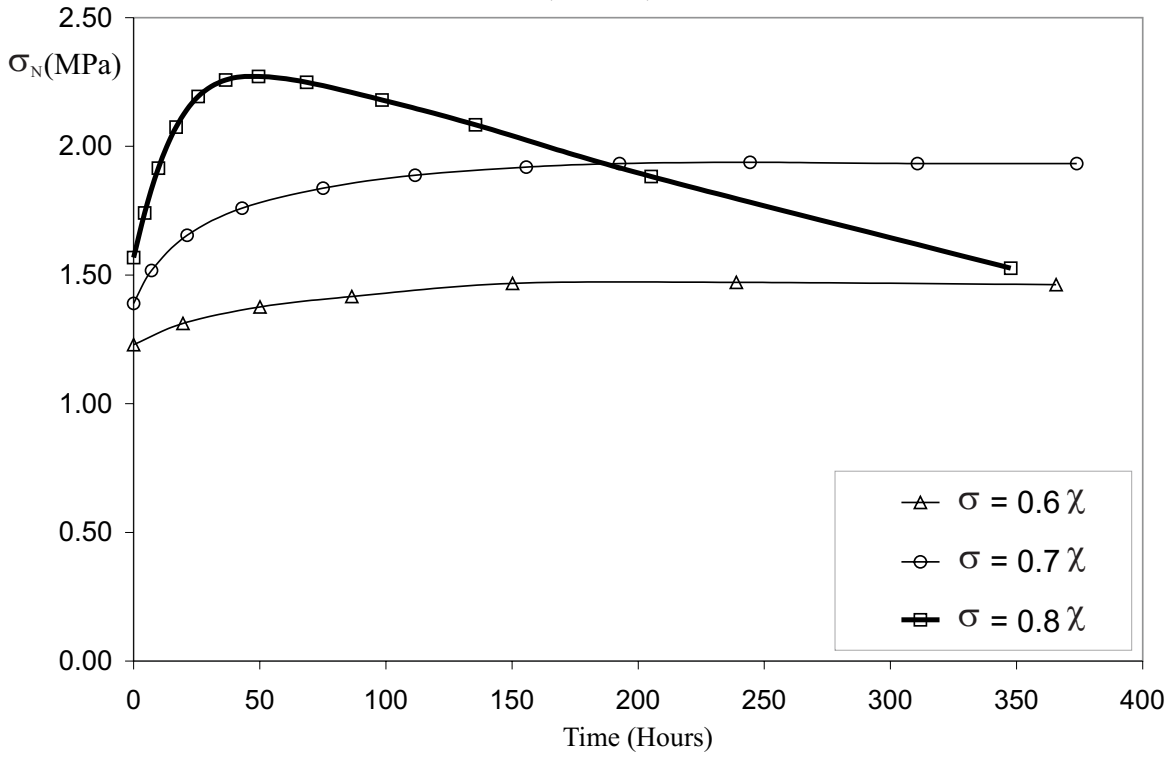

Figure 12: Creep test - Stress evolution with time for various stress levels

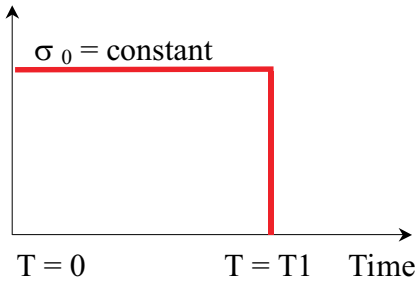

Figure 13: Creep test – Unloading scheme

The responses for both, the unloading and reloading cases are plotted in figure 14. It is clear that after the load has been removed the model experienced elastic unloading and the remaining deformation is plastic. In the unloading case the elastic deformation is given as $\Delta u = \Delta\sigma/E_N$, where $\Delta\sigma$ is the portion of unloading stress. The reloading cases are also plotted in the same figure. Again consider the same model as before, which is now loaded at time t = 0 hours with the same initial load as before; subsequently at time $t = t_1$ hours this load is increased adding a $\Delta\sigma = 0.03\chi$, 0.08χ and 0.15χ. For the lower reloading levels, the delayed displacements remains bounded, but are unbounded for the higher stress level. As we explain previously, this fact corresponds to a negative viscoplastic modulus. This case represents the so-called delayed rupture. The last example in this series of uniaxial creep tests explores this behavior further. Again consider the same model as before, which is now loaded at time t = 0 hours with an initial load P =1.20 KN; subsequently at time t = 245 hours this load is increased applying $\Delta P = 0.2$ KN. Figure 15 illustrate model behavior in this case.

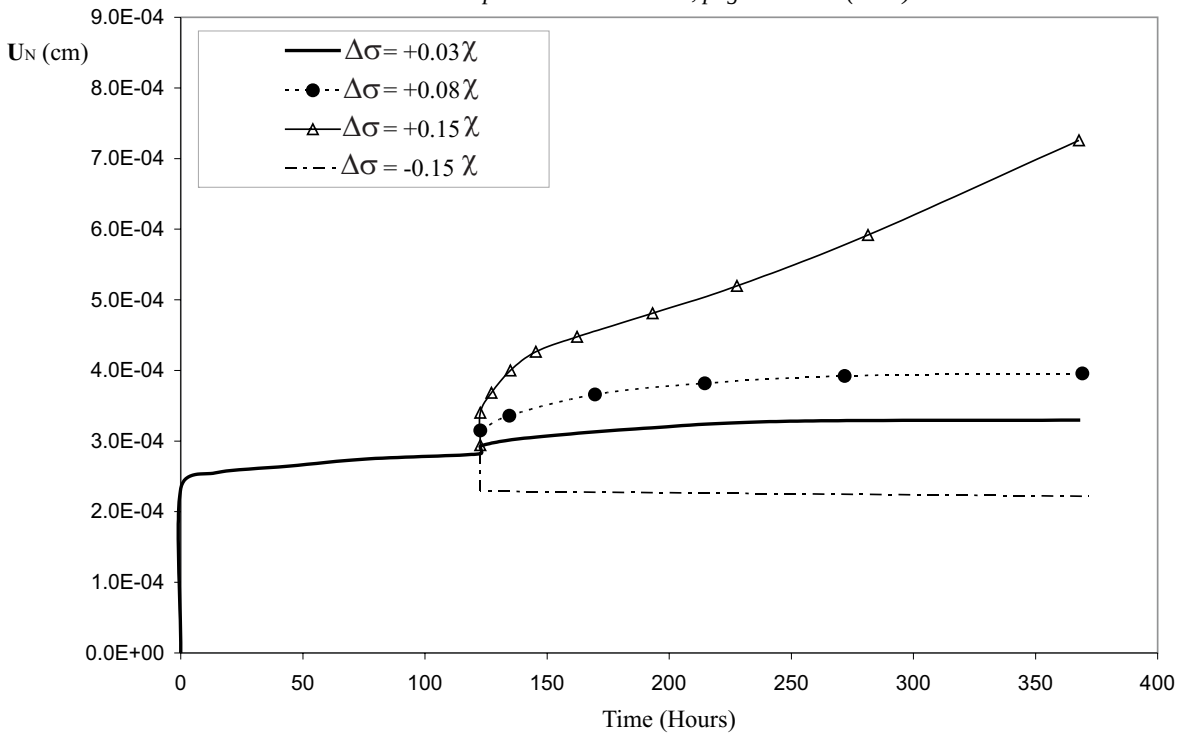

Figure 14: Creep test - Unloading/reloading cases for $\sigma = 0.6\chi$

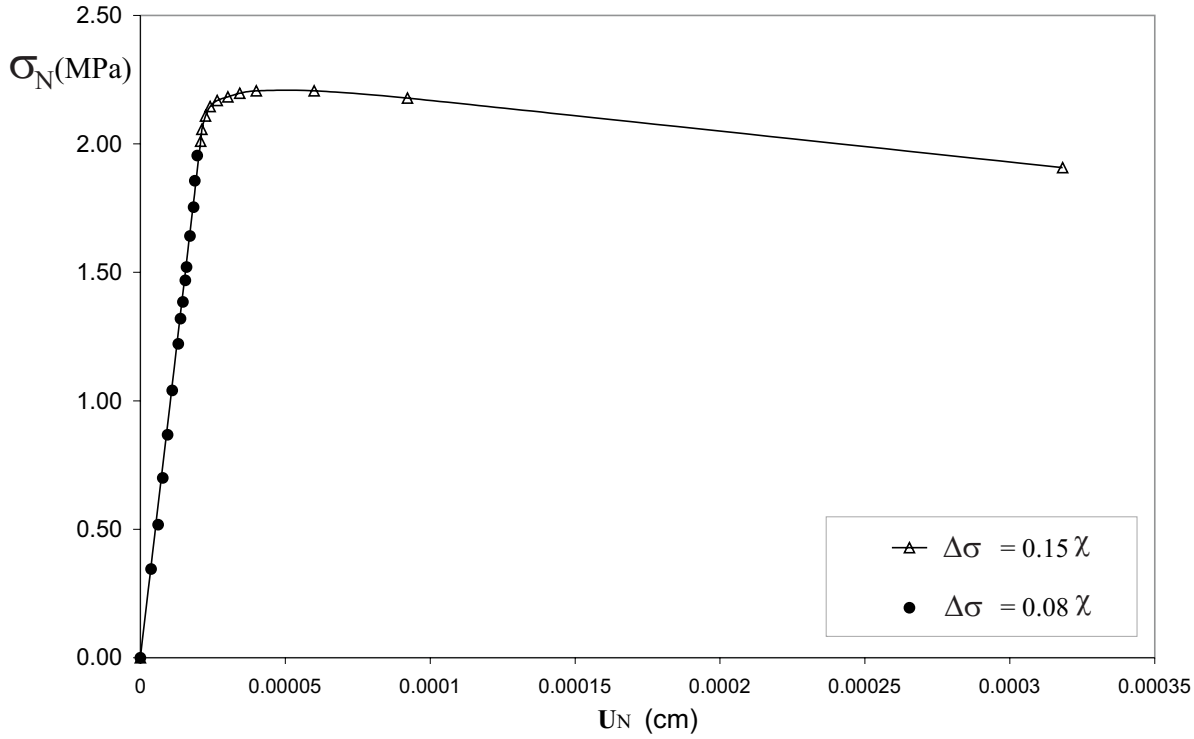

Figure 15: Stress-displacement curve for the reloading cases

In the same figure the case in which a load P=1.40 KN is applied from the beginning is included. In both loadcases, the displacements are tending to the corresponding elastoplastic limits within increasing time, which have been also computed and plotted. These results show a good agreement with the observed behavior of real materials under step-loading conditions.

5. CONCLUSIONS

From the presented results, we see that when assuming very long term phenomena, a simple elastoplastic model may work sufficiently, but when this is not the case, a viscoplastic model can provide better results, and can approach the material behavior in a more realistic way. In fact, in many cases and with certain materials, elasto-viscoplastic models are the only way to reproduce the experimental measurements. From the developed examples, a relevant distinction arise between elastoplastic and viscoplastic formulations, and is the fact that an elastoplastic model implies that the plastic deformations are immediately fully developed. On the other hand, using a viscoplastic model, one has the possibility to split different phases into different loadcases, and study the significance of the time gap between them. Therefore, the options during analysis are further enhanced. Finally, an outcome of great importance too, is that by using a viscoplastic material modelling, the overall Finite Element Algorithm becomes more stable and experiences less convergence problems. The fact that stresses above the yield limit are allowed and not ruled out as in classical plasticity, eliminates the limitations and restrictions, that may otherwise be sources of instabilities, and since the viscoplastic model reaches the elastoplastic solution in the limit, as it was shown in the simple case studies, applying viscoplastic modelling for rate-independent problems, results in numerically stabilizing the solution process. On the other hand, the rate-dependent version of the interface model by Carol et al. for the analysis of quasi-brittle or heterogeneous materials has been tested in the low velocities or quasi-static regime. Numerical simulations of creep and relaxation cases were successfully performed at constitutive level. The obtained results demonstrate model capabilities to reproduce in a realistic manner the observed behavior of a wide range of engineering, rate-dependent materials. The presented interface formulation seems to be a suitable numerical tool to model a wide range of rate-dependent problems, like crack growth under sustained loads, stress relaxation, cyclic loading and stage construction in the context of a mesomechanic or discrete approach to the fracture of mortar and concrete structures.

6. REFERENCES

Carol, I., Prat, P. and Lopez, C.M., A Normal/ Shear Cracking Model. Interface Implementation for Discrete Analysis. *Journal of Enginnering Mechanics*, *ASCE*, 123(8), pp. 765-773, 1997.

Carosio, A., Viscoplasticidad Continua y Consistente. *Tesis doctoral, Laboratorio de Estructuras - Univ. Nac. De Tucumán*, Argentina, 2001.

Carosio, A., Willam, K. and Etse, G., On the Consistency of Viscoplastic Formulations. *International Journal of Solids and Structures*, Vol. 37, pp. 7349-7369, 2000.

Cristescu N., Viscoplasticity of Geomaterials. *Visco-Plastic Behavior of Geomaterials. Springer-Verlag*, New York, 103-207, 1994.

Cristescu N., Cazacu, O., Viscoplasticity of geomaterials. *Modelling in Geomechanis.* Wiley, Sussex, 129 -154, 2000.

Desai, C.S., Zhang, D., Viscoplastic Models for Geologic Materials with Generalized Flow Rule. *International Journal for Numerical and Analytical Methods in Geomechanics*, 11, 603-620, 1987.

Etse, G., Carosio, A. and Willam, K., Limit State and Localization of Perzyna Viscoplastic Material. *Int. Journal on Cohesive and Frictional Materials,* (23), 1, pp. 32-42, 1997.

Etse, G., Willam, K., Failure Analysis of Elastoviscoplastic Material Models. *Journal of Engng. Mechanics*, (125), 1, pp. 60-69, 1999.

Etse, G., Lorefice, R., Carosio, A. and Carol, I., Rate Dependent Interface Model Formulation for Quasi-Brittle Materials. *Proc. International Conference on Fracture Mechanics of Concrete Structures - FRAMCOS 5*. Boulder, Colorado, USA, pp. 301-305, 2004.

Etse, G., Lorefice, R., López, C.M. and Carol, I., Meso and Macromechanic Approaches for Rate Dependent Analysis of Concrete Behavior. *International Workshop in Fracture Mechanics of Concrete Structures*. Vail, Colorado, USA, 2004.

Johansson M., Mahnken R., Runesson K., Efficient Integration Technique for Generalized Viscoplasticity Coupled to Damage. *International Journal for Numerical Methods in Engineering*, 44, 1727-1747, 1999.

López Garello, C.M., Análisis Microestructural de la Fractura del Hormigón Utilizando Elementos Tipo Junta. Aplicación a diferentes Hormigones. *Tesis doctoral, Universitat Politécnica de Catalunya*, Barcelona, Spain, 1999.

Lorefice, R., Etse, G., C.M. Lopez and I. Carol, Mesomechanic Analysis of Time Dependent Concrete Behavior. *EURO-C 2006, Computational Modeling of Concrete Structure*s. Mayrhofen, Austria, (2006).

Lorefice, R., Etse, G., Rizo Patron, M., Influencia de la Tasa de Deformacion en el Creep y Relajacion de Hormigones Normales. *ENIEF 2007, Cordoba, Argentina, 2007.*

Lorefice, R., Modelación de la Respuesta Dinámica del Hormigón Mediante los Criterios Meso y Macromecánicos. *Tesis Doctoral*, *CEMNCI - Univ. Nac. De Tucuman*, 2007.

Lorefice, R., Etse, G., and Carol, I., Viscoplastic Approach for Rate-Dependent Failure Analysis of Concrete Joints and Interfaces. *International Journal of Solids and Structures* 45, 2686–2705, 2008.

Mahnken R., Johansson M., Runesson K., Parameter Estimation for a Viscoplastic Damage Model Using a Gradient-Based Optimization Technique. *Engineering Computations*, 15, 925-955, 1998.

Perzyna, P., The Constitutive Equations for Rate Sensitive Materials. *Quarter of Applied Mathematics*, Vol. 20, pp. 321-332, 1963.

Perzyna, P., Fundamental Problems in Viscoplasticity. *Advances in Applied Mechanics 9*, pp. 244-368, 1966.

Ponthot, J.P., Radial Return Extensions for Viscoplasticity and Lubricated Friction. *Proc. International Conference on Structural Mechanics and Reactor Technology SMIRT-13*. Porto Alegre, Brazil, Vol. 2, pp. 711-722, 1995.

Ristinmaa M., Ottosen N. S., Consequences of Dynamic Yield Surface in Viscoplasticity. *International Journal of Solids and Structures*, 37, 4601-4622, 2000.

Runesson, K., Constitutive Theory and Computational Technique for Dissipative Materials. *Lecture notes*, Goteborg, Sweden, 1996.

Simo J. C., Strain Softening and Dissipation: a unification of approaches. *Cracking and Damage, Strain Localization and Size Effects*, Mazars J., Bazant Z. P., (Editors). Elsevier, London, 440-461, 1989.

Simo, J.C., Hughes, T.J.R., Elastoplasticity and Viscoplasticity. Computational aspects. *Springer-Verlag*, Berlin, 1998.

Sluys, J.L., Wave Propagation and Dispersion in Softening Solids. *PhD Thesis, TU-Delft*. The Netherlands, 1992.

Wang, W.M., Stationary and Propagative Instabilities in Metals-A Computational Point of View". *PhD Thesis. TU-Delft*. The Netherlands, 1997.

Wang, W.M., Sluys, L.J., de Borst, R., Viscoplasticity for instabilities due to strain softening and strain-rate softening. *International Journal for Numerical Methods in Engineering*, 40, 3839-3864, 1997.

Willam, K. Etse, G. Munz, T., Localized Failure in Elastic - Viscoplastic Materials. *Proc. Concreep 5*, Barcelona, Ed. Z. P. Bazant and I. Carol, F. N. Spon, London, pp. 327-344, 1993.